Russian Chemical Bulletin, International Edition, Vol. 59, No. 2, pp. 361—370, February, 2010

New tin(IV) *o*-iminosemiquinone complexes

A. V. Piskunov,★ I. N. Meshcheryakova, E. V. Baranov, G. K. Fukin, V. K. Cherkasov, and G. A. Abakumov

G. A. Razuvaev Institute of Organometallic Chemistry, Russian Academy of Sciences,
49 ul. Tropinina, 603950 Nizhny Novgorod, Russian Federation.
Fax: +7 (831) 462 7497. E-mail: pial@iomc.ras.ru

New tin(IV) mono- and bis-*o*-iminosemiquinone complexes were obtained by the exchange reaction of radical anion lithium salt of 4,6-di-*tert*-butyl-*N*-(2,6-diisopropylphenyl)-*o*-iminobenzoquinone with tin(IV) organochlorides. The compounds synthesized were characterized by EPR spectroscopy and X-ray diffraction analysis. Substituents on the tin atom were found to affect stability of paramagnetic metal derivatives formed.

Key words: *o*-iminosemiquinone complexes, tin, electron paramagnetic resonance, X-ray diffraction analysis.

o-Semiquinone ligands are widely used as spin labels in the study of coordination and organometal compounds.[1—7] EPR spectra of these derivatives give plethora of information on composition, structure, and dynamics of the metal coordination sphere. Tin(IV) complexes containing ligands based on the radical anion *o*-quinone ligands are widely studied by both Russian[6,8—11] and foreign[12—14] scientists. At the same time, most of tin(IV) paramagnetic derivatives obtained earlier have been studied only in solution and have not been isolated in the individual state. There are only several examples of the structurally characterized tin(IV) *o*-semiquinone complexes.[15,16] The synthesis of organotin derivatives containing, along with a paramagnetic ligand, alkyl and aryl substituents on the metal atom is complicated by the secondary processes of bimolecular elimination of a hydrocarbon radical.[11,14] Recently,[17,18] we have shown that a replacement of the *o*-semiquinone ligand with its nitrogen-containing analog, *o*-iminosemiquinone, allows one to obtain stable mono- and biradical compounds with phenyl substituents on the metal atom.

The present work is a continuation of this study and is devoted to the synthesis of tin(IV) *o*-iminosemiquinone complexes containing, along with a paramagnetic ligand, alkyl and aryl substituents, as well as to the study of compounds synthesized by EPR spectroscopy and X-ray diffraction analysis.

Results and Discussion

Compounds synthesized in this work were obtained by the exchange reaction of tin(IV) organochlorides with radical anion lithium salt of 4,6-di-*tert*-butyl-*N*-(2,6-diisopropylphenyl)-*o*-iminobenzoquinone (imSQLi) in 60—80% yields (Scheme 1).

Complexes **1—4**, **6—10**, **12**, and **14** were obtained for the first time. The synthesized derivatives **5**, **11**, and **13** (see Scheme 1) in their elemental analysis data, IR and EPR spectroscopic data are identical to the compounds described earlier,[17,18] which were obtained by the oxidation-reduction transformations involving diphenyl- and diethyltin(IV) 4,6-di-*tert*-butyl-*N*-(2,6-diisopropylphenyl)-*o*-amidophenolates. The structures of compounds **1**, **2**, **7**, **9**, and **12** were established by X-ray diffraction analysis.

The reaction of imSQLi with tin(IV) triorganochlorides in equimolar proportion in THF takes place at room temperature and is completed over several minutes, during which the reaction mixture acquires green color. The solutions obtained have well resolved signals in the EPR spectra. For complexes **1—4**, they are doublet (1 : 1) of triplets (1 : 1 : 1) due to the interaction of the unpaired electron with the nuclei ^{14}N (99.63%, $I = 1$, $\mu_N = 0.4037$) and ^{1}H (99.98%, $I = 1/2$, $\mu_N = 2.7928$)[19] with the satellite splitting on the tin magnetic isotopes ^{117}Sn (7.68%, $I = 1/2$, $\mu_N = 1.000$) and ^{119}Sn (8.58%, $I = 1/2$, $\mu_N = 1.046$)[19] (Fig. 1, *a*, *b*). Parameters of the EPR spectra are given in Table 1. Triphenyl (**1**) and trimethyl (**2**) derivatives were successfully isolated in the individual states by crystallization from hexane. The compounds are stable on exposure to oxygen and atmospheric moisture in the crystalline state and rapidly decompose when their solutions are exposed to air. The complexes are paramagnetic in both solution and crystalline state.

In the case of triethyl- and tributyltin chlorides, trialkyl derivatives **3** and **4** are primary reaction products as well. This is confirmed by the green color of the solution and the EPR spectra (see Fig. 1, *b*), which are similar to the EPR spectra of complexes **1** and **2**. However, the green color of the solution turned brown and the signal in the

Published in Russian in *Izvestiya Akademii Nauk. Seriya Khimicheskaya,* No. 2, pp. 354—363, February, 2010.

1066-5285/10/5902-0361 © 2010 Springer Science+Business Media, Inc.

Scheme 1

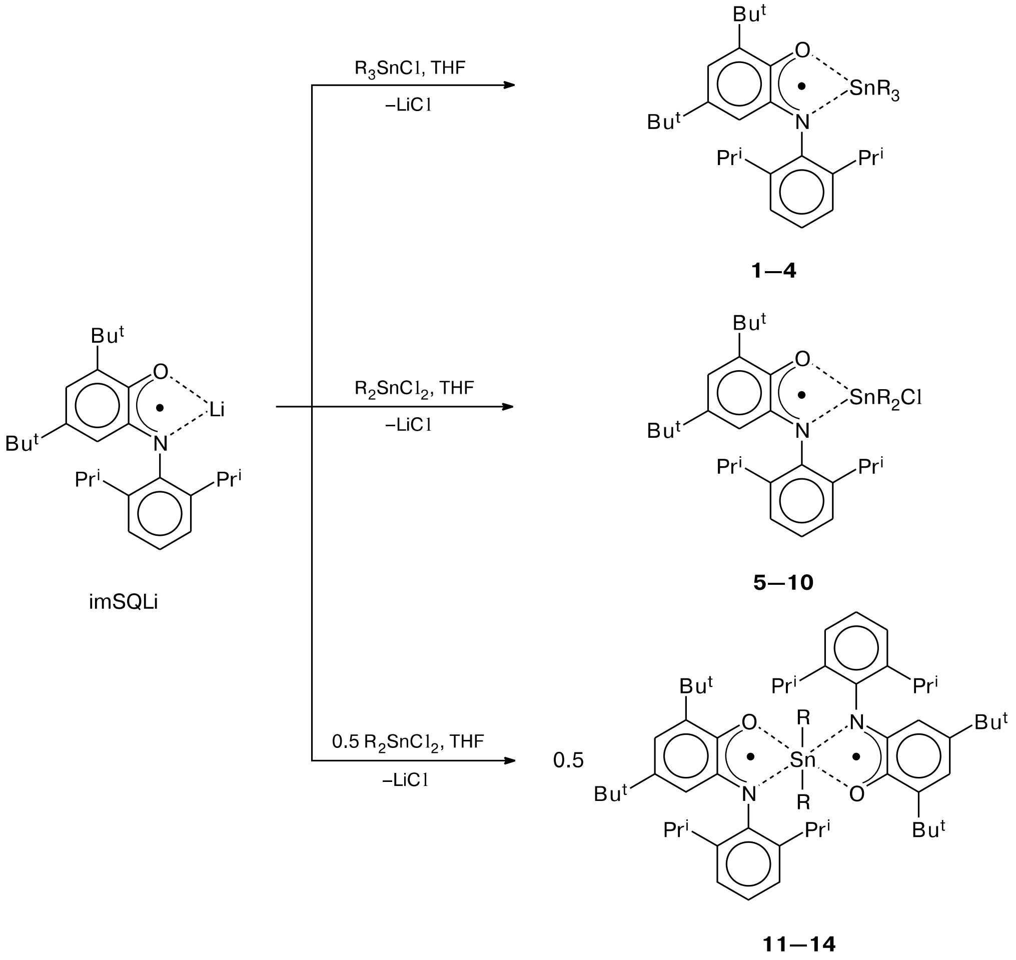

R = Ph (**1**, **5**, **11**), Me (**2**, **6**, **12**), Et (**3**, **7**, **13**), Bu^n (**4**, **8**, **14**), Bu^t (**9**), PhCH$_2$ (**10**)

EPR spectrum disappears with time. We failed to isolate and characterize diamagnetic products of transformation of complexes **3** and **4**. GC-MS analysis of the gas phase over the solution of decomposed complex imSQSnEt$_3$ showed the absence of gaseous hydrocarbons, ethane, ethylene, and butane. The absence of ethylene in the decomposition products indicates that no β-elimination occurs during decomposition of the complex. There is neither elimination of the ethyl radical into the solution, which is indicated by the absence of ethane and butane among the reaction products.

Table 1. Parameters of the EPR spectra of complexes **1**—**10** (hexane, T = 285 K)

Complex	$a_i(^1H)$	$a_i(^{14}N)$	$a_i(^{117,119}Sn)$	g_i
	mT			
1	0.34	0.56	2.33	2.0036
2	0.29	0.54	2.56	2.0026
3	0.32	0.56	2.48	2.0040
4	0.31	0.56	2.57	2.0033
5	0.42	0.58	3.72	2.0028
6	0.39	0.60	4.03	2.0027
7	0.40	0.59	4.20	2.0028
8	0.40	0.60	4.29	2.0032
9	0.44	0.62	5.07	2.0024
10	0.41	0.59	4.47	2.0039

The use of tin diorganodichlorides as the starting reactants in equimolar proportion with imSQLi succeeded in isolation of a whole series of paramagnetic *o*-iminosemiquinone derivatives **5**—**10** (see Scheme 1) irrespective of the nature of the hydrocarbon substituent on the tin atom. The EPR spectra of complexes **5**—**10** and derivatives **1**—**4** are characterized by the interaction of the unpaired electron with the magnetic isotopes ^{14}N, ^{1}H, ^{117}Sn, and ^{119}Sn (see Fig. 1, *c*). Parameters of the EPR spectra are given in Table 1. The absence in the EPR

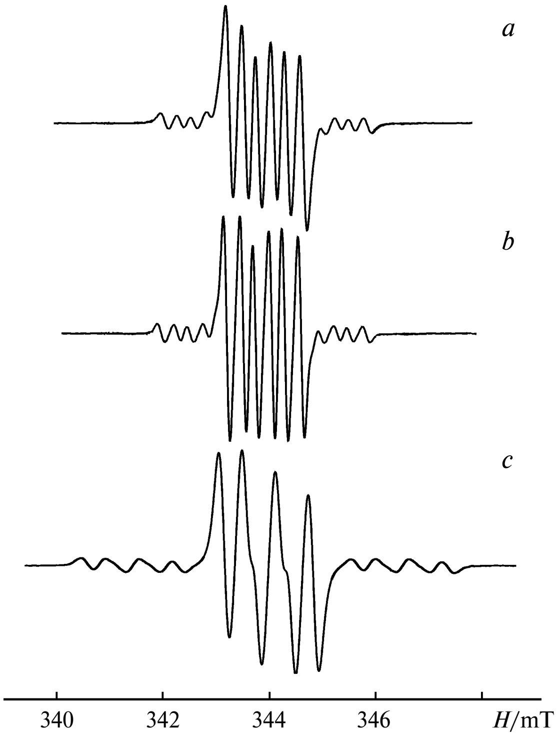

Fig. 1. Isotropic EPR spectra of complexes **2** (*a*), **3** (*b*), and **9** (*c*) in hexane at $T = 290$ K.

Scheme 2

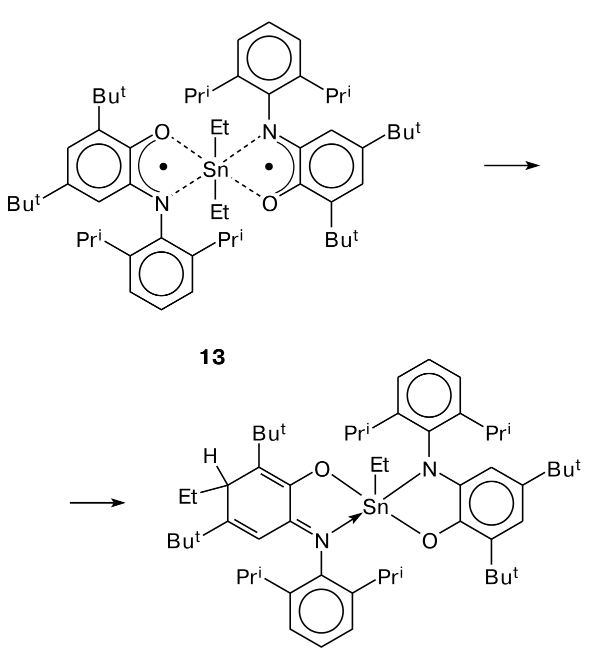

13

15

spectra of compounds **5—10** (see Fig. 1, *c*) of the hyperfine interaction of the unpaired electron with the magnetic isotopes of chlorine atom ^{35}Cl and ^{37}Cl indicates that the halogen atom is in the same plane with the *o*-iminosemiquinolate ligand. The X-ray diffraction data (see below) are in good agreement with this.

The reaction of imSQLi with R_2SnCl_2 in the ratio 2 : 1 (see Scheme 1) leads to biradical complexes **11—14**. Complexes **11** and **12** were isolated in the individual state. The biradical products with the ethyl (**13**) and *n*-butyl (**14**) substituents on the tin atom can be identified only in solution by EPR (Fig. 2). These compounds, as well as monoradical derivatives **3** and **4**, are labile under the reaction conditions and, as it was shown using complex **13** as an example,**[18]** rearrange to yield diamagnetic complexes (Scheme 2).

The anisotropic EPR spectra of compounds **11—14** (see Fig. 2) have the form characteristic of biradicals, that confirms the presence of two *o*-iminosemiquinolate ligands in them. The anisotropic EPR spectra have the following parameters of splitting in the zero field: D = 20.9 mT, E = 0.6 mT (**11**), D = 19.7 mT, E = 1.6 mT (**12**) in the 2-methyltetrahydrofuran matrix; D = 21.9 mT, E = 0.6 mT (**13**), D = 21.1 mT, E = 0.6 mT (**14**) in the toluene matrix.

The reaction of imSQLi with $Bu^t_2SnCl_2$ in the molar ratio 2 : 1 results in the isolation of tin compound, which according to the EPR spectroscopic data is the complex **9** with one *o*-iminoquinone ligand. Probably, the fact that the product of this reaction is the mono-, rather than biradical tin derivative, is explained by considerable steric hindrance for the introduction of the second *o*-iminoquinone ligand into the metal coordination surrounding already containing two bulky *tert*-butyl substituents.

Molecular structure of complexes 1, 2, 7, 9, and 12. Crystals of compounds suitable for X-ray diffraction anal-

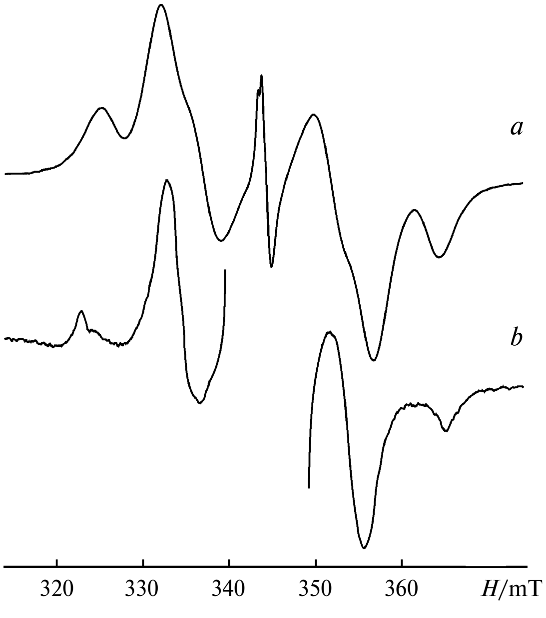

Fig. 2. Anisotropic EPR spectra of complexes **12** (*a*) and 14 (*b*) at $T = 140$ K.

ysis were obtained by the slow crystallization from acetone (complex **1**) and hexane (complexes **2**, **7**, **9**, and **12**). Molecular structures of the complexes are shown in Figs 3—7. Selected bond distances and bond angles are given in Tables 2 and 3. The crystallographic data, parameters of the X-ray diffraction experiments and refinement are collected in Table 4.

The crystal cell of compound **1** contains 0.5 of solvate molecule of acetone per one independent molecule of the complex. The tin atom in complexes **1**, **2**, **7**, and **9** has similar distorted trigonal-bipyramidal surrounding.

In the apical positions, there are atom O(1) of the *o*-iminosemiquinone ligand and atoms C(39) and C(29) for complexes **1** and **2**, respectively, or atom Cl(1) for complexes **7** and **9**. The bipyramid plane is formed by the atoms N(1) and C of the alkyl (aryl) substituents on the tin atom. The atom Sn(1) comes out of the bipyramid plane by 0.312, 0.409, 0.200, and 0.209 Å for complexes **1**, **2**, **7**, and **9**, respectively. The chlorine atom in complexes **7** and **9** are close to the plane of the *o*-iminosemiquinone chelate ring. The deviation of the atom Cl(1) from the plane O(1)Sn(1)N(1)C(2)C(1) is 0.115 and 0.086 Å for complexes **7** and **9**, respectively.

The presence of two unsymmetric chelate rings leads to the formation of two isomers in the tin six-coordinated complex **12**. Both isomeric molecules are present in the crystal cell (see Fig. 7, *a*). Since the bond distances and

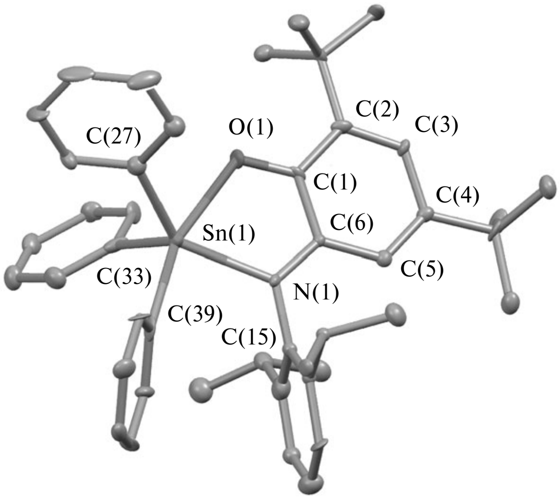

Fig. 3. Molecular structure of complex **1**. Thermal ellipsoids of 50% probability are given. Hydrogen atoms are not shown.

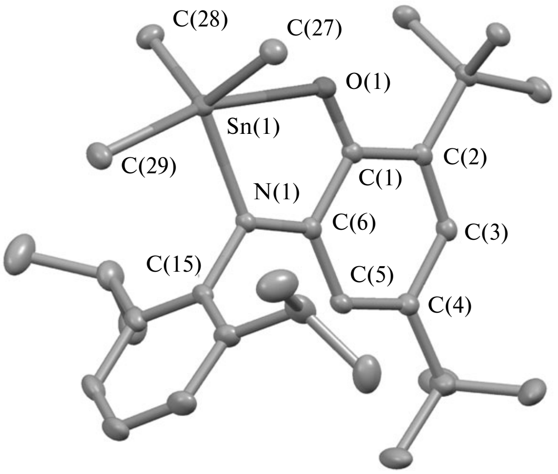

Fig. 4. Molecular structure of complex **2**. Thermal ellipsoids of 50% probability are given. Hydrogen atoms are not shown.

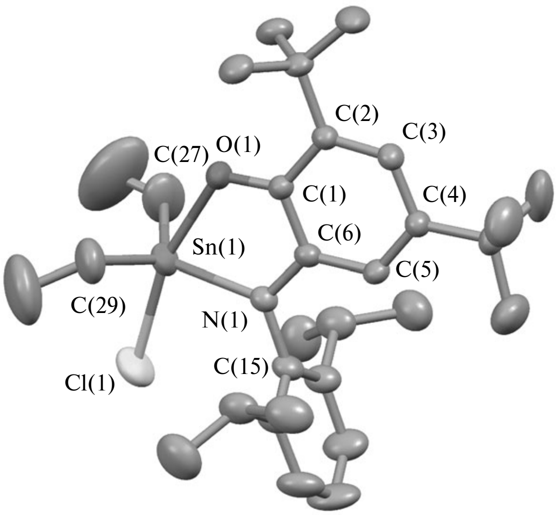

Fig. 5. Molecular structure of complex **7**. Thermal ellipsoids of 50% probability are given. Hydrogen atoms are not shown.

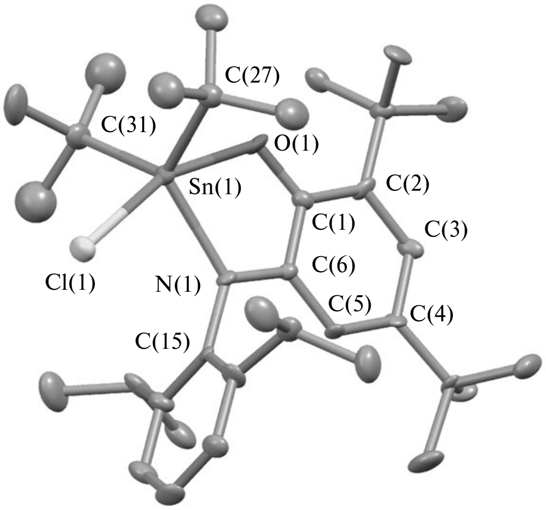

Fig. 6. Molecular structure of complex **9**. Thermal ellipsoids of 50% probability are given. Hydrogen atoms are not shown.

Table 2. Selected bond distances (*d*) and bond angles (ω) for complexes **1**, **2**, **7**, and **9**

Bond	*d*/Å			
	1	**2**	**7**	**9**
Sn(1)—N(1)	2.2073(18)	2.1609(13)	2.140(3)	2.186(8)
Sn(1)—O(1)	2.2381(15)	2.3937(11)	2.210(2)	2.235(8)
Sn(1)—Cl(1)	—	—	2.4291(13)	2.457(3)
O(1)—C(1)	1.286(3)	1.2719(19)	1.274(4)	1.322(7)
N(1)—C(2)	1.336(3)	1.343(2)	1.345(4)	1.342(9)
N(1)—C(15)	1.439(3)	1.4355(19)	1.451(4)	1.477(8)
C(1)—C(2)	1.455(3)	1.458(2)	1.451(4)	1.390(10)
C(1)—C(6)	1.438(3)	1.444(2)	1.427(4)	1.390(10)
C(2)—C(3)	1.419(3)	1.421(2)	1.415(5)	1.390(10)
C(3)—C(4)	1.363(3)	1.367(2)	1.354(4)	1.390(10)
C(4)—C(5)	1.434(3)	1.434(2)	1.428(5)	1.390(10)
C(5)—C(6)	1.371(3)	1.371(2)	1.367(5)	1.390(10)
Sn(1)—C(27)	2.157(2)	2.1698(17)	2.151(6)	2.1479(13)
Sn(1)—C(28)	—	2.1349(17)	—	—
Sn(1)—C(29)	—	2.1318(17)	2.126(5)	—
Sn(1)—C(31)	—	—	—	2.1791(14)
Sn(1)—C(33)	2.146(2)	—	—	—
Sn(1)—C(39)	2.178(2)	—	—	—

Angle	ω/deg			
	1	**2**	**7**	**9**
O(1)—Sn(1)—N(1)	71.99(6)	70.31(4)	73.95(9)	72.8(3)
O(1)—Sn(1)—Cl(1)	—	—	164.25(8)	161.5(2)
N(1)—Sn(1)—Cl(1)	—	—	90.35(8)	88.7(2)
C(1)—O(1)—Sn(1)	117.63(13)	114.87(9)	116.06(19)	114.9(4)
C(2)—N(1)—Sn(1)	117.88(14)	121.47(10)	116.9(2)	116.9(5)
C(15)—N(1)—Sn(1)	121.93(13)	119.44(10)	125.1(2)	124.2(5)
C(15)—N(1)—C(2)	119.40(18)	119.07(13)	117.9(3)	118.8(6)
O(1)—Sn(1)—C(27)	83.92(7)	164.51(6)	89.2(2)	88.7(2)
O(1)—Sn(1)—C(28)	—	83.70(6)	—	—
O(1)—Sn(1)—C(29)	—	82.38(6)	89.40(16)	—
O(1)—Sn(1)—C(31)	—	—	—	92.2(2)
O(1)—Sn(1)—C(33)	92.96(7)	—	—	—
O(1)—Sn(1)—C(39)	158.07(7)	—	—	—
N(1)—Sn(1)—C(27)	135.46(8)	94.22(6)	113.8(2)	120.2(2)
N(1)—Sn(1)—C(28)	—	115.07(6)	—	—
N(1)—Sn(1)—C(29)	—	111.39(6)	116.13(18)	—
N(1)—Sn(1)—C(31)	—	—	—	119.0(2)
N(1)—Sn(1)—C(33)	109.91(7)	—	—	—
N(1)—Sn(1)—C(39)	92.31(8)	—	—	—

angles in both molecules are close, we will discuss only molecule A. The six-coordinated tin atom in complex **12** is in the distorted octahedron surrounding formed by two chelate *o*-iminosemiquinone ligands and two methyl groups. The equatorial plane is formed by atoms O(1), O(2), C(53), and C(54), atoms N(1) and N(2) are in the

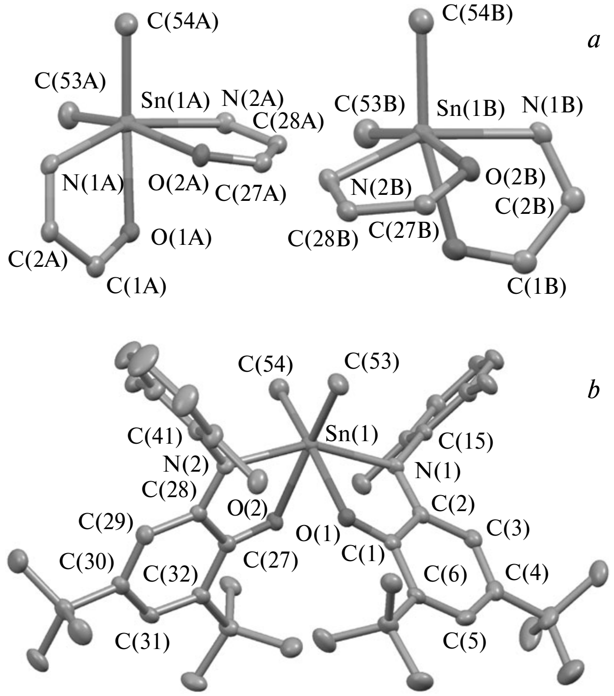

Fig. 7. Fragments of two independent molecules of the crystal cell of complex **12** (*a*) and molecular structure of complex **12A** (*b*). Thermal ellipsoids of 50% probability are given. Hydrogen atoms and Me groups of the isopropyl substituents are not shown.

Table 3. Selected bond distances (*d*) and bond angles (ω) for complex **12**

Bond	*d*/Å
Sn(1)—N(1)	2.2366(11)
Sn(1)—O(1)	2.1973(9)
O(1)—C(1)	1.2875(16)
N(1)—C(2)	1.3354(16)
N(1)—C(15)	1.4348(17)
C(1)—C(2)	1.4563(18)
C(1)—C(6)	1.4342(18)
C(2)—C(3)	1.4202(18)
C(3)—C(4)	1.3659(19)
C(4)—C(5)	1.425(2)
C(5)—C(6)	1.3819(19)
Sn(1)—C(53)	2.1499(15)
Sn(1)—C(54)	2.1588(14)
Sn(1)—N(2)	2.2281(11)
Sn(1)—O(2)	2.2010(9)
O(2)—C(27)	1.2988(15)
N(2)—C(28)	1.3377(16)
N(2)—C(41)	1.4386(16)
C(27)—C(28)	1.4547(18)
C(27)—C(32)	1.4265(18)
C(28)—C(29)	1.4189(18)
C(29)—C(30)	1.3723(19)
C(30)—C(31)	1.4201(19)
C(31)—C(32)	1.3894(18)

Angle	ω/deg
O(1)—Sn(1)—N(1)	73.08(4)
C(1)—O(1)—Sn(1)	117.08(8)
C(2)—N(1)—Sn(1)	115.27(8)
C(15)—N(1)—Sn(1)	125.54(8)
C(15)—N(1)—C(2)	119.14(11)
O(1)—Sn(1)—C(53)	90.54(5)
O(1)—Sn(1)—C(54)	161.98(5)
N(1)—Sn(1)—C(53)	100.93(5)
N(1)—Sn(1)—C(54)	95.24(5)
O(2)—Sn(1)—N(2)	73.38(4)
C(27)—O(2)—Sn(1)	116.84(8)
C(28)—N(2)—Sn(1)	115.82(8)
C(41)—N(2)—Sn(1)	125.19(8)
C(28)—N(2)—C(41)	118.84(11)
O(2)—Sn(1)—C(53)	162.21(5)
O(2)—Sn(1)—C(54)	90.11(5)
N(2)—Sn(1)—C(53)	94.81(5)
N(2)—Sn(1)—C(54)	100.60(5)
C(53)—Sn(1)—C(54)	105.39(6)
O(1)—Sn(1)—O(2)	75.69(3)
N(1)—Sn(1)—N(2)	153.84(4)
O(1)—Sn(1)—N(2)	86.10(4)
O(2)—Sn(1)—N(1)	85.99(4)

Table 4. Crystallographic data, parameters of X-ray diffraction experiments and refinement for complexes **1**, **2**, **7**, **9**, and **12**

Complex	**1**·0.5Me_2CO	**2**	**7**	**9**	**12**
Formula	$C_{45.5}H_{55}NO_{1.5}Sn$	$C_{29}H_{46}NOSn$	$C_{30}H_{47}ClNOSn$	$C_{34}H_{55}ClNOSn$	$C_{54}H_{80}N_2O_2Sn$
M	758.60	543.36	591.83	647.93	907.89
T/K	100(2)	100(2)	293(2)	298(2)	100(2)
Crystal system	Monoclinic	Triclinic	Monoclinic	Monoclinic	Monoclinic
Space group	*P*2(1)/*c*	$P\bar{1}$	*P*2(1)/*n*	*C*2/*c*	*P*2(1)
a/Å	10.3362(3)	11.0927(3)	10.2949(7)	20.431(4)	18.7586(5)
b/Å	14.7718(4)	11.1861(3)	14.6967(10)	10.773(2)	12.2051(3)
c/Å	25.8275(6)	12.8913(3)	21.2852(15)	31.027(7)	22.3614(6)
α/deg	90	88.9530(10)	90	90	90
β/deg	99.3030(10)	74.2920(10)	101.019(2)	90.880(4)	91.3070(10)
γ/deg	90	70.322(10)	90	90	90
V/Å^3	3891.59(18)	1445.24(6)	3161.1(4)	6828(2)	5118.3(2)
Z	4	2	4	8	4
d_{calc}/g cm^{-3}	1.295	1.249	1.244	1.261	1.178
μ/mm^{-1}	0.692	0.903	0.913	0.851	0.538
F(000)	1588	570	1236	2728	1936
Crystal size/mm	0.15×0.14×0.06	0.20×0.18×0.12	0.15×0.10×0.08	0.23×0.22×0.18	0.27×0.24×0.18
Range of measurements, θ/deg	1.59—26.50	2.64—27.00	1.69—25.00	1.31—24.00	0.91—27.50
Intervals of indices of reflections	$-12 \le h \le 12$, $-18 \le k \le 18$, $-32 \le l \le 32$	$-14 \le h \le 13$, $-14 \le k \le 11$, $-12 \le l \le 16$	$-9 \le h \le 12$, $-17 \le k \le 17$, $-25 \le l \le 23$	$-23 \le h \le 23$, $-12 \le k \le 12$, $-35 \le l \le 35$	$-24 \le h \le 24$, $-15 \le k \le 15$, $-29 \le l \le 29$
Number of reflections	34322	9516	17217	22902	49345
Number of independent reflections	8049	6280	5541	5255	23195
R_{int}	0.0499	0.0106	0.0246	0.0690	0.0191
Reliability (F^2)	1.006	1.058	1.050	1.232	1.053
R_1/wR_2 ($I > 2\sigma(I)$)	0.0353/0.0778	0.0225/0.0572	0.0452/0.1208	0.1548/0.3426	0.0273/0.0636
R_1/wR_2 (from all parameters)	0.0549/0.0830	0.0242/0.0581	0.0617/0.1285	0.1653/0.3469	0.0306/0.0649
Residual electron density (max/min)/e Å^{-3}	1.178/−0.420	1.128/−0.315	0.835/−0.618	4.537/−2.914	1.232/−0.656

apical positions. The dihedral angle between the planes of the radical ligands is 61.87°, which is somewhat larger than in analogous complex containing phenyl substituents on the metal atom (57.02°).[18] The distance between the centroid *o*-iminosemiquinone ligands (5.197 Å) is in good agreement with the distance between radical centers calculated[20] for this complex based on the parameters of anisotropic EPR spectrum (5.20 Å). The methyl groups are in *cis*-position with respect to each other, the angle C(53)—Sn(1)—C(54) is 105.39(6)°. At the same time, the chelate ligands are arranged so that the nitrogen atoms are in *trans*-position and the angle N(1)—Sn(1)—N(2) is equal to 153.84(4)° (see Fig. 7, *b*).

In accordance with the radical anion state, a characteristic distribution of the bond distances is observed in *o*-iminoquinone ligands of complexes **1**, **2**, **7**, **9**, and **12**. The distances C—O (1.2719(19)—1.322(7) Å) and C—N (1.3354(16)—1.345(4) Å) are in the range typical of the metal *o*-iminosemiquinone complexes.[21] For the six-membered ring C(1)—C(6) in the molecules of the complexes under study (as well C(27)—C(32) in complex **12**), a quinoid type of distortion is present characteristic of *o*-semiquinones[22] and *o*-iminosemiquinones,[21] which is reflected in alternation of the C—C bond distances. For instance, the distances C(1)—C(2), C(1)—C(6), C(2)—C(3), and C(4)—C(5) are in the range 1.415(5)—1.458(2) Å and considerably longer than the bonds C(3)—C(4) and C(5)—C(6) (1.354(4)—1.3819(19) Å).

The bond distances Sn—O (2.1973(9)—2.3937(11) Å) and Sn—N (2.140(3)—2.2366(11) Å) in complexes under consideration are somewhat larger than the sum of the covalent radii for the corresponding elements (2.11 and 2.12 Å),[23] that is characteristic of the coordination of *o*-iminoquinone radical anions with tin.[17,18]

We analyzed relationship between the structure of obtained tin *o*-iminosemiquinone complexes and their stability. According to the literature data,[11,18] the loss of the free valence in the radical of the tin(IV) *o*-semiquinone and *o*-iminosemiquinone complexes containing alkyl and aryl substituents on the metal atom occurs by the homolytic cleavage of the metal—carbon bond. In this case, the loss in energy is balanced by the formation of two regular covalent Sn—O or Sn—N bonds during further formation of the corresponding catecholate or amidophenolate derivatives. In accordance with this, the stability of the paramagnetic complexes should increase with the increase in energy of the Sn—C bond for different hydrocarbon substituents. Thus, tetraalkyl- and tetraphenyl-substituted stannanes form the following order in energy of the Sn—C bond: Ph (259±8 kJ mol^{-1})[24] > Me (222±4 kJ mol^{-1})[24] > Bu^n (197±8 kJ mol^{-1})[24] ≈ Et (192±4 kJ mol^{-1})[24]. These data are in good agreement with the fact that the tin *o*-iminosemiquinone complexes with phenyl substituents on the metal atom are stable in both crystal state and solution upon heating to 100 °C.[18] Analogous methyl-substituted compounds are stable in solution at room temperature for several weeks, however, upon heating above 100 °C in toluene they decompose to diamagnetic derivatives over several hours. Paramagnetic complexes based on ethyl- and butyl-substituted tin undergo rapid transformation already at room temperature and, as a result, it is impossible to isolate them in the individual state under usual conditions.

We performed calculations by the DFT method[25—28] for complexes **1**, **2**, **7** and unstable in solution complex **3**, as well as the corresponding radicals $Ph^{\cdot}$, $Me^{\cdot}$, $Et^{\cdot}$, and $imSQSnR_2^{\cdot}$, to evaluate energy of the Sn—R bond in the tin *o*-iminosemiquinone complexes. Energy of the Sn—C bond in the tin *o*-iminosemiquinone complexes changes in the following order of substituents: Ph (195.136 kJ mol^{-1}) > > Me (145.165 kJ mol^{-1}) > Et (125.086 kJ mol^{-1}) and agrees with analogous tendency of the bond weakening in tetraalkyl- and tetraphenyl-substituted stannanes. Note that the Sn—Et bond energy in unstable complex **3** (125.086 kJ mol^{-1}) is considerably lower than in its monochloride analog **7** (182.623 kJ mol^{-1}), in which it is comparable with the Sn—Ph bond energy in complex **1**. To sum up, the replacement of the ethyl group with the chlorine atom in complex **7** increases the strength of the Sn—Et bond and, consequently, stabilizes the complex. It is possible that the increase in energy of the Sn—alkyl bond upon replacement of one of the alkyl groups by the chlorine atom going from derivatives **3** and **4** to derivatives **7**—**10** is an important factor determining stability of the tin paramagnetic complexes.

In addition, it is of interest to analyze stability of the complexes not only from the point of view of the Sn—alkyl bond energy, but also from the point of view of steric factors. For the quantitative evaluation of the latter, it was suggested[29,30] to use a degree of filling of the metal coordination sphere (*G*) in the complex formed. For the calculation of the degree of filling of coordination sphere in complexes **1**, **2**, **7**, **9**, and **12**, there were used geometric characteristics from the X-ray diffraction data obtained in the present study. The geometric characteristics of complexes **5**,[17] **11**, and **15** [18] were taken from the works published earlier. For unstable complexes **3** and **13** and model compounds $imSQSn(Bu^t)_3$ (**16**) and $imSQ_2Sn(Bu^t)_2$ (**17**), the molecular structures were calculated by methods of molecular mechanics using the HyperChem 7.01 program.[31] To develop molecular structures of complexes **3**, **13**, **16**, and **17**, we used the bond distance values of analogous complexes **9** and **12**. Optimization of the geometry was performed in the coordination sphere of the Sn atom under conditions of the fixed bond distances Sn—C (2.14 Å) corresponding to the sum of the covalent radii of Sn and C atoms. According to this optimization, the distances Sn—N and Sn—O insignificantly changed as compared to the analogous values in similar complexes **9** and **12**. The optimized geometry of the molecular structure of unstable complex **3** was as well obtained from the DFT calculations when the Sn—C bond energy was calculated. Geometries of complex **3** optimized by various methods insignificantly differ from each other, the degree of filling differing within ~2%. Thus, the use of the data on optimization of geometry of complexes **13**, **16**, and **17** by molecular mechanics for the evaluation of parameter *G* is justified, since calculations by the method of density functional for them is very complicated. Methyl-substituted complex **2** has the lowest degree of filling of the metal coordination sphere (*G*) among mono-*o*-iminosemiquinone complexes of tris-alkyl derivatives (Table 5). Parameter *G* for unstable complex **3** is significantly higher, that should lead to the increase in nonvalent repulsion between the ligands of the complex and, consequently, to additional weakening of the Sn—C bond. At the same time, when one of the alkyl substituents is replaced with the chlorine atom, the degree of filling of the coordination sphere decreases (going from complexes **1**, **3**, and **16** to complexes **5**, **7**, and **9**, respectively). Along with higher bond energy, this can also promote an increase in stability of the monochlorinated complexes **5**—**10** as compared to their tris-alkyl analogs.

Table 5. Degree of filling of the metal coordination sphere (*G*) in tin *o*-iminosemiquinone complexes **1**—**3**, **5**, **7**, **9**, **11**—**13**, and **15**—**17**

Complex	*G* (%)	Complex	*G* (%)
1	82.2(2)	**11**	94.6(2)
2	79.0(2)	**12**	91.1(2)
3	86.8(2), 84.1(2)*	**13**	96.1(2)
5	80.9(2)	**15**	91.9(2)
7	80.1(2)	**16**	94.4(2)
9	86.7(2)	**17**	98.3(2)

* Calculation based on the geometry optimized by the DFT method.

Similar situation is also observed in the series of bis-*o*-iminosemiquinone complexes. Methyl-substituted complex **12** has the lowest degree of filling of the metal coordination sphere, whereas unstable six-coordinated complex **13** (G = 96.1(2)%) undergoes rearrangement to the five-coordinated complex **15**, which is characterized by considerably lower steric hindrance of the coordination center (G = 91.9(2)%). The complex with two *tert*-butyl substituents on the tin atom (**17**) should have 98.3(2)% filling of the metal coordination sphere. As a result, the exchange reaction between imSQLi and $Bu^t{}_2SnCl_2$ proceeds only when the ratio of reactants is 1 : 1, and no introduction of the second *o*-iminosemiquinone fragment occurs.

It should be emphasized that the model complex **16** (G = 94.4(2)%) is not formed in the reaction, whereas complex **11** with the same degree of filling of the coordination space is an individual compound (G = 94.6(2)%). This is due to the fact that the Sn—Bu^t bond energy in complex **16** is lower than the Sn—Ph bond energy in complex **11**, therefore, the steric factors cannot interfere with the formation of complex **11**. In addition, as it has been already noted above, complex **13** (G = 96.1(2)%) undergoes rearrangement to complex **15** resulting in the reduction of parameter G to 91.9(2)%. Consequently, in this case the steric factors have a dominating influence on stability, like in the case of hypothetical complexes **16** and **17**. Judging from the value of parameter G, the degree of filling of the coordination sphere in these complexes is high, therefore, the major nonvalent interactions in them are ligand-to-ligand intramolecular interactions in the metal coordination sphere. However, considerable reduction of steric factors can cause dramatic change in stability and, as a result, the complex structures. The lowering the degree of shielding the metal atom can lead to both the formation of the associate structures due to the metal—ligand intermolecular interactions and the reactions (rearrangements) in the coordination sphere due to the presence of free space there, which results in the increase of parameter G of the complex. In another words, for the optimal stability of the complex, a balance between steric and energy factors is necessary.

In conclusion, in the course of the present study a series of paramagnetic tin complexes based on sterically hindered *o*-iminoquinone were synthesized. An order of stability of compounds obtained was established depending on the nature of substituents bonded to the tin atom. It was shown that stability of derivatives under study is determined by both the tin—carbon bond energy and the degree of filling of the metal coordination sphere.

Experimental

All the experiments on the synthesis and study of tin(IV) *o*-iminosemiquinolate complexes were performed under reduced pressure in the absence of oxygen and moisture traces.

IR spectra were recorded on a FSM-1201 IR Fourier-spectrometer in Nujol and KBr pellets. EPR spectra were recorded on a Bruker EMX spectrometer. Diphenylpicrylhydrazyl (g = 2.0037) was used as a standard in determination of g-factor.

Solvents were dried and purified according to the known procedures.[32] Organotin compounds R_3SnCl and R_2SnCl_2 (R = = Me, Et, Bu^n, Bu^t, $PhCH_2$, Ph) were obtained according to the known procedures.[33]

Lithium *o*-iminosemiquinolate was synthesized by treatment of lithium 4,6-di-*tert*-butyl-*N*-(2,6-diisopropylphenyl)-*o*-amidophenolate[17] with equimolar amount of 4,6-di-*tert*-butyl-*N*-(2,6-diisopropylphenyl)-*o*-iminobenzoquinone[34] in THF, during which the reaction mixture turned color from red to deep blue. The solution obtained was used in further syntheses *in situ*.

Complexes 1—14 (general procedure). A solution of lithium *o*-iminosemiquinolate (0.5 mmol) in THF (20 mL) was slowly added to a solution of organotin halide (0.5 mmol for complexes **1—10** and 0.25 mmol for complexes **11—14**) in the same solvent (10 mL), the reaction mixture turned color from bright blue to dark green. The solution obtained was stirred for 30 min at room temperature followed by evaporation of the solvent at reduced pressure. The residue was treated with hexane (40 mL) and filtered through a Shott glass filter No. 4. The hexane solution was half concentrated and slowly cooled to −18 °C. The crystals of tin *o*-iminosemiquinone complexes formed were decanted from the mother liquor and dried at reduced pressure.

Complexes **5** and **11** have been described earlier.[17,18] Compounds **1**, **2**, **6—9**, and **12** were isolated in the individual state and characterized for the first time. Derivatives **3**, **4**, **10**, **13**, and **14** were characterized in solution by EPR spectroscopy.

Compounds **1**, **2**, **6—9**, and **12** are stable on exposure to oxygen and air moisture in crystalline state. Solid samples decompose without melting on heating above 140 °C. They are soluble in most organic solvents and in solution rapidly decompose in air.

[4,6-Di-*tert*-butyl-*N*-(2,6-diisopropylphenyl)-*o*-iminosemiquinolato]triphenyltin(IV) (1). The yield was 72.8%. Found (%): C, 73.05; H, 6.95; Sn, 15.97. $C_{44}H_{49}NOSn$. Calculated (%): C, 72.73; H, 6.80; Sn, 16.34. IR, ν/cm^{-1}: 1584 s, 1336 m, 1317 m, 1252 s, 1166 m, 1112 w, 1073 s, 995 s, 912 m, 868 s, 798 s, 727 v.s, 698 v.s, 627 w, 498 m, 457 w, 447 w.

[4,6-Di-*tert*-butyl-*N*-(2,6-diisopropylphenyl)-*o*-iminosemiquinolato]trimethyltin(IV) (2). The yield was 74.5%. Found (%): C, 65.80; H, 8.34; Sn, 21.31. $C_{29}H_{52}NOSn$. Calculated (%): C, 64.46; H, 8.02; Sn, 21.97. IR, ν/cm^{-1}: 1584 s, 1484 m, 1357 m, 1340 w, 1252 s, 1198 m, 1178 w, 1109 w, 1053 w, 1026 w, 993 m, 934 w, 911 m, 878 w, 861 m, 797 m, 770 m, 625 w, 540 s, 511 m, 496 s.

[4,6-Di-*tert*-butyl-*N*-(2,6-diisopropylphenyl)-*o*-iminosemiquinolato]dimethyltin(IV) chloride (6). The yield was 61.6%. Found (%): C, 59.63; H, 7.04; Cl, 6.25; Sn, 21.37. $C_{28}H_{40}ClNOSn$. Calculated (%): C, 59.97; H, 7.19; Cl, 6.32; Sn, 21.17. IR, ν/cm^{-1}: 1581 s, 1454 w, 1441 w, 1359 w, 1336 w, 1319 w, 1253 m, 1200 w, 1171 w, 1108 w, 1027 w, 993 m, 936 w, 916 w, 888 m, 879 w, 865 m, 797 s, 778 s, 663 w, 631 w, 556 m.

[4,6-Di-*tert*-butyl-*N*-(2,6-diisopropylphenyl)-*o*-iminosemiquinolato]diethyltin(IV) chloride (7). The yield was 71.5%. Found (%): C, 60.42; H, 7.93; Cl, 5.60; Sn, 20.34. $C_{30}H_{47}ClNOSn$. Calculated (%): C, 60.88; H, 8.00; Cl, 5.99; Sn, 20.06. IR, ν/cm^{-1}: 1583 s, 1457 w, 1438 w, 1357 w, 1337 w, 1255 m, 1200 w, 1170 w, 1111 w, 1100 w, 1054 m, 1029 w, 993 m, 963 w, 938 w, 916 w, 887 m, 880 w, 864 m, 798 s, 779 s, 679 w, 663 w, 576 m.

[4,6-Di-*tert*-butyl-*N*-(2,6-diisopropylphenyl)-*o*-iminosemiquinolato]dibutyltin(IV) chloride (8). The yield was 61.3%. Found (%): C, 63.45; H, 9.08; Sn, 17.63; Cl, 5.23. $C_{35}H_{59}ClNOSn$. Calculated (%): C, 63.31; H, 8.96; Sn, 17.88; Cl, 5.34. IR, ν/cm^{-1}: 1582 s, 1469 s, 1455 s, 1441 s, 1388 m, 1359 m, 1336 m, 1318 m, 1292 w, 1254 m, 1220 w, 1199 m, 1171 m, 1110 m, 1100 m, 1078 w, 1054 w, 1028 m, 994 m, 935 s, 914 w, 887 m, 877 m, 864 m, 824 w, 798 m, 779 w, 767 m, 745 w, 706 w, 695 w, 665 w, 652 w, 631 w, 611 w, 557 w, 540 w, 529 w, 510 w, 500 w, 476 w, 457 w, 437 w.

[4,6-Di-*tert*-butyl-*N*-(2,6-diisopropylphenyl)-*o*-iminosemiquinolato]di-*tert*-butyltin(IV) chloride (9). The yield was 65.8%. Found (%): C, 63.43; H, 8.21; Cl, 5.56; Sn, 18.48. $C_{34}H_{52}ClNOSn$. Calculated (%): C, 63.32; H, 8.13; Cl, 5.50; Sn, 18.41. IR, ν/cm^{-1}: 1586 s, 1468 s, 1437 s, 1382 s, 1365 s, 1332 m, 1320 m, 1251 s, 1198 m, 1115 w, 1100 m, 1055 w, 1028 m, 1016 m, 992 m, 935 w, 913 m, 869 s, 823 w, 802 s, 771 m, 665 w, 629 w, 497 w.

Bis[4,6-di-*tert*-butyl-*N*-(2,6-diisopropylphenyl)-*o*-iminosemiquinolato]dimethyltin(IV) (12). The yield was 79.5%. Found (%): C, 70.82; H, 8.14; Sn, 13.35. $C_{54}H_{74}N_2O_2Sn$. Calculated (%): C, 71.91; H, 8.27; Sn, 13.16. IR, ν/cm^{-1}: 1580 s, 1431 m, 1379 m, 1332 m, 1250 s, 1200 m, 1168 m, 1055 w, 993 m, 933 w, 912 m, 866 s, 823 w, 797 s, 767 m, 663 w, 625 w, 518 w, 498 w.

X-ray diffraction analysis. X-ray diffraction study was performed on a Smart Apex diffractometer (Mo-Kα-irradiation, a graphite monochromator). Structures were solved by the direct method with subsequent refinement by the full-matrix mean-squares method from F^2 using the SHELXTL program.[35] Allowance for absorption was made using the SADABS programs.[36] All the nonhydrogen atoms were refined in anisotropic approximation. Hydrogen atoms in complexes **1**, **2**, **7**, and **9** were placed in the geometrically calculated positions and refined using the riding model. In complex **12**, the hydrogen atom positions were found from the differential synthesis and refined with the isotropic thermal parameters, excluding hydrogen atoms of one *tert*-butyl group of the *o*-iminosemiquinone ligand, which were placed in the geometrically calculated positions and refined using the riding model. In the crystal of complex **1**, a solvate molecules of acetone were found, which were disordered over two positions with respect to the inversion center.

The structure of complex **12** was solved in noncenter symmetric space group *P*2(1). Analysis of the systematic data using the XPREP program showed the presence of only the screw axis of the second order 2(1). An average value $|E^*E - 1| = 0.707$ testifies in favor of the space group *P*2(1), which is close to the analogous value (0.736) suggested for the noncenter symmetric group, but considerably lower than the value $|E^*E - 1| = 0.968$ probable for the center symmetric space group. To confirm the correctness of the choice of the group *P*2(1), we solved the structure **12** in center symmetric space group *P*2(1)/*c* with one independent molecule of complex **12**, however, the refinement reached the *R*-factor of ~20% ($wR_2 \approx 66\%$). This was the reason to choose the variant of the noncenter symmetric group *P*2(1).

Quantum chemical calculations. Geometries of complexes **1**, **2**, **3**, and **7** were optimized using the ORCA program[37] the B3LYP functional in the DGDZVP basis. The absence of imaginary frequencies suggests that the molecules are in the minimum of potential energy.

This work was financially supported by the Russian Foundation for Basic Research (Project Nos 07-03-00711-a, 07-03-00819-a, and 06-03-32728-a) and the Council on Grants at the President of the Russian Federation (Program of State Support for Leading Scientific Schools and Young Scientists of the Russian Federation, Grant NSh 4182.2008.3 and MK-1286.2009.3).

References

1. G. A. Abakumov, *Mendeleev Zh. Khim.*, 1979, 156 [*Mendeleev Chem. J.* (*Engl. Transl.*), 1979].
2. V. I. Nevodchikov, G. A. Abakumov, V. K. Cherkasov, G. A. Razuvaev, *J. Organomet. Chem.*, 1981, **214**, 119.
3. G. A. Abakumov, V. K. Cherkasov, K. G. Shalnova, I. A. Teplova, G. A. Razuvaev, *J. Organomet. Chem.*, 1982, **236**, 333.
4. G. A. Abakumov, A. V. Krashilina, V. K. Cherkasov, L. N. Zakharov, *Dokl. Akad. Nauk*, 2003, **391**, 343 [*Dokl. Chem.* (*Engl. Transl.*), 2003, **391**, 185].
5. K. A. Kozhanov, M. P. Bubnov, V. K. Cherkasov, G. K. Fukin, G. A. Abakumov, *J. Chem. Soc.*, *Dalton Trans.*, 2004, 2957.
6. Z. K. Kasymbekova, A. I. Prokof´ev, N. N. Bubnov, S. P. Solodovnikov, M. I. Kabachnik, *Dokl. Akad. Nauk SSSR*, 1982, **263**, 352 [*Dokl. Chem.* (*Engl. Transl.*), 1982, 263].
7. G. A. Abakumov, V. K. Cherkasov, A. V. Piskunov, N. O. Druzhkov, *Dokl. Akad. Nauk*, 2004, **399**, 353 [*Dokl. Chem.* (*Engl. Transl.*), 2004, **399**, 223].
8. M. I. Kabachnik, N. N. Bubnov, A. I. Prokof´ev, S. P. Solodovnikov, *Sci. Rev. B*, 1981, **3**, 197.
9. N. V. Berezina, V. K. Cherkasov, V. P. Maslennikov, *Zh. Obshch. Khim.*, 1996, **66**, 1488 [*Russ. J. Gen. Chem.* (*Engl. Transl.*), 1996, **66**, 1451].
10. G. A. Razuvaev, V. A. Tsarjapkin, L. V. Gorbunova, V. K. Cherkasov, G. A. Abakumov, E. S. Klimov, *J. Organomet. Chem.*, 1979, **174**, 47.
11. G. A. Razuvaev, G. A. Abakumov, P. Ya. Bayushkin, V. A. Tsaryapkin, V. K. Cherkasov, *Izv. Akad. Nauk SSSR, Ser. Khim.*, 1984, 2098 [*Bull. Acad. Sci. USSR, Div. Chem. Sci.* (*Engl. Transl.*), 1984, **33**, 1915].
12. A. G. Davies, J. A. Hawari, *J. Organomet. Chem.*, 1983, **251**, 53.
13. H. B. Stegmann, R. Schrade, H. Saur, P. Schuler, K. Scheffler, *J. Organomet. Chem.*, 1981, **214**, 197.
14. M. A. Brown, B. R. McGarvey, A. Ozarowsky, D. G. Tuck, *J. Organomet. Chem.*, 1998, **550**, 165.
15. A. S. Batsanov, J. A. K. Howard, M. A. Brown, B. R. McGarvey, D. G. Tuck, *Chem. Commun.*, 1997, 699.
16. G. A. Abakumov, V. K. Cherkasov, A. V. Piskunov, A. V. Lado, G. K. Fukin, E. V. Baranov, *Dokl. Akad. Nauk*, 2006, **410**, 57 [*Dokl. Chem.* (*Engl. Transl.*), 2006, **410**, 145].
17. I. A. Aivaz´yan, A. V. Piskunov, G. A. Abakumov, V. K. Cherkasov, O. V. Kuznetsova, G. K. Fukin, E. V. Baranov, *Izv. Akad. Nauk, Ser. Khim.*, 2007, 253 [*Russ. Chem. Bull., Int. Ed.*, 2007, **56**, 261].
18. A. V. Piskunov, I. N. Mescheryakova, G. K. Fukin, E. V. Baranov, M. Hummert, A. S. Shavyrin, V. K. Cherkasov, G. A. Abakumov, *Chem. Eur. J.*, 2008, **14**, 10085.
19. J. Emsley, *The Elements*, Clarendon Press, Oxford, 1991, 251 pp.
20. A. Carrington, A. D. McLachlan, *Introduction to Magnetic Resonance, with Applications to Chemistry and Chemical Physics*, Harper and Row, New York—London, 1967, 266 pp.

21. A. I. Poddelskii, V. K. Cherkasov, G. A. Abakumov, *Coord. Chem. Rev.*, 2009, **253**, 291.
22. C. G. Pierpont, R. M. Buchanan, *Coord. Chem. Rev.*, 1981, **38**, 45.
23. S. S. Batsanov, *Zh. Inorg. Khim.*, 1991, **36**, 3015 [*J. Inorg. Chem. USSR (Engl. Transl.)*, 1991, **36**, 1694].
24. I. B. Rabinovich, V. P. Nistratov, V. I. Tel´noi, M. S. Sheiman, *Termodinamika metalloorganicheskikh soedinenii* [*Thermodynamics of Organometallic Compounds*], Nizhegorod. Univ. Publ., N. Novgorod, 1996, 297 pp. (in Russian).
25. J. Chalupský, F. Neese, E. I. Solomon, U. Ryde, L. Rulíšek, *Inorg. Chem.*, 2006, **45**, 11051.
26. S. Sinnecker, F. Neese, *J. Comput. Chem.*, 2006, **27**, 1463.
27. M. Wanko, M. Hoffmann, P. Strodel, W. Thiel, F. Neese, T. Frauenheim, M. Elstner, *J. Phys. Chem. B*, 2005, **109**, 3606.
28. J. Schöneboom, F. Neese, W. Thiel, *J. Am. Chem. Soc.*, 2005, **127**, 5840.
29. I. A. Guzei, M. Wendt, *J. Chem. Soc., Dalton Trans.*, 2006, 3991.
30. I. A. Guzei, M. Wendt, *Program Solid-G*, Madison, WI, USA, 2004.
31. *HyperChem(TM) Professional 7.01*, Hypercube, Inc., 1115 NW 4th Street, Gainesville, Florida 32601, USA.
32. A. J. Gordon, R. A. Ford, *The Chemist´s Companion*, Wiley Intersci. Publ., New York, 1972, 537 pp.
33. K. A. Kocheshkov, N. N. Zemlyanskii, N. I. Sheverdina, E. M. Panov, *Methody elementoorganicheskoi khimii. Germanii. Olovo. Svinets* [*Methods of Organometallic Chemistry. Germanium. Tin. Lead*], Nauka, Moscow, 1968, 704 (in Russian).
34. G. A. Abakumov, N. O. Druzhkov, Yu. A. Kurskii, A. S. Shavyrin, *Izv. Akad. Nauk, Ser. Khim.*, 2003, 682 [*Russ. Chem. Bull.*, *Int. Ed.*, 2003, **52**, 712].
35. G. M. Sheldrick, *SHELXTL v. 6.12, Structure Determination Software Suite*, Bruker AXS, Madison, Wisconsin, USA, 2000.
36. G. M. Sheldrick, *SADABS v.2.01, Bruker/Siemens Area Detector Absorption Correction Program*, Bruker AXS, Madison, Wisconsin, USA, 1998.
37. F. Neese, *ORCA — an ab initio, Density Functional and Semiempirical Program Package, Version 2.3, Revision 09*, Max Planck Institut für Strahlenchemie, Mülheim, Germany, 2004.

Received December 8, 2008;
in revised form July 9, 2009